 CMES, vol.33, no.1, pp.17-47, 2008

Integration of Shell FEA with Geometric Modeling on NURBS Surface Representation for Practical Applications

Maenghyo Cho[1], Jinbok Choi[2] and Hee Yuel Roh[3]

Abstract: The framework for the linkage between geometric modeling and an analysis based on the NURBS technology is developed in this study. In the present study, The NURBS surfaces were generated by interpolating a given set of data points or by extracting the necessary information to construct the NURBS surface from the IGES format file which was generated by the commercial CAD systems. Numerical examples showed the rate of displacement convergence for the various parameter-izations of the NURBS surface. Quadric surface, which is generated exactly by NURBS representation, was considered. One of the important advantages of the NURBS equation is its ability for exact mathematical expression of quadric shape curves or surfaces. A trimmed surface, which is often encountered during a modeling process in the CAD systems is also presented in this study. The performance of the shell element that is based on Naghdi shell theory integrated with exact geometric representations by the NURBS equation were compared to that of a previously reported FE shell elements in the selected benchmark problems.

Keyword: Shell, NURBS, Finite element method, Geometric modeling.

1 Introduction

The shell finite element can be classified into two categories: the three-dimensional solid-based elements and shell theory-based elements. A degenerated shell element is one of the elements which are based on a three- dimensional solid model[Ahmad S, Irons BM, Zienkiewicz OC (1970)]. This element has been very popular over the past several decades because it is not based on complicated shell theories. Surface geometric properties such as those described by a curvature tensor do not have to be introduced in this formulation. A degenerated shell element can be used to

[1] Professor, School of Mechanical and Aerospace Engineering, Seoul National University, Seoul, Korea
[2] School of Mechanical and Aerospace Engineering, Seoul National University, Seoul, Korea
[3] Project I T/F Team, Digital Printing Division, Samsung Electronics, Korea

model an arbitrary shape of a shell surfaces because the surface can be constructed by interpolating nodal values through the iso-parametric mapping, whereas a shell theory-based element can handle the bending-stretching coupling properly, but it cannot easily be applied to model an arbitrary shape of a shell surfaces. So, a shell theory-based element can be applied only for specific shell surfaces with relatively simple geometry. But in practical problems, usually, shell surfaces are not presented in a closed analytical form. For this reason, a shell theory-based element has difficulties in application to the general shell surfaces. And recently, there is an alternative way of using the meshless computational method in the analysis of shell structure.[Sladek,J.et al. (2006); T.Jarak et al. (2007)].

Surfaces can be identified by several ways for shell finite element analysis. First, exact analytical surface expressions such as cylinder or hemisphere can be given. In this case, shell surface geometric quantities can be directly extracted in the analysis without any geometric errors. But, as mentioned above, it is not always possible to represent general surfaces in an exact closed form. Second, surfaces can be generated by interpolating or approximating a set of given points. Generally, we can obtain the digitized coordinate values of points by scanning. Because the NURBS equation provides interpolation or approximation methods, the fitting surfaces which we want for the analysis can be easily obtained. For the more practical applications, geometric surface generation can be generated by the modeling process provided by the CAD system. Most current commercial CAD systems employ the NURBS technology to model and manipulate surfaces. The NURBS is the generalized form of a non-rational B-spline and rational and non-rational Bezier curves and surfaces. In addition, it can generate and manipulate surfaces, for example, by providing a mathematical basis for representing analytical shapes such as conic sections and quadratic surfaces. That is, it can exactly express the quadratic (or quadric)surfaces such as cylindrical, conical, spherical, paraboloidal and hyperboloidal surfaces. More details about the NURBS technology [Les Piegl, Wayne Tiller (1997), G. Farin (1993) and C. De Boor (1972)]. Furthermore, the NURBS algorithms are fast and stable and they enable us to design surfaces intuitively. Because of these merits of the NURBS, it has been the industrial standard for design and data exchange of geometric information. Many national or international standards, for example, IGES, STEP etc., recognize the NURBS as a powerful tools for geometric design.

The shell theory-based element which was developed by Manenghyo Cho, Hee Yuel Roh (2003) has a two-parameter representation in the surfaces. And all the geometric computations can be performed in a local surface patch. So, if a shell surface such as the Cosserat surface[J.C. Simo, D.D. Fox (1989), J.C. Simo, D.D. Fox, S. Rafai (1989)] used in shell theory-based element are represented by two param-

eters, the shell theory-based element may be used in the analysis of an arbitrary-shape shell structure. This developed element also employed the assumed strain method to avoid locking problems and the performance was improved by using bubble function displacements. [Keejoo Lee et al. (2002), Y. Basar and O.Kintzel (2003)]

The NURBS surfaces are usually represented by two parameters in the parametric domain. As mentioned above, the surfaces in CAD systems are usually generated by using NURBS representation and the blending functions of NURBS surfaces are composed by two parameters defined in a local region. A general tensor-based shell element has a two-parameter representation in the shell surfaces, and all geometric computations can be performed in the local surface patch. Naturally, the NURBS surface function could be directly linked to the shell analysis routine. We can obtain more "geometrically-exact" surface quantities for the analysis by using the shell theory-based element than by using the solid-based element. The concept for integrating the shell FE analysis with CAD geometric modeling was proposed in our previous works [Hee Yuel Roh and Maenghyo Cho, (2004, 2005)]. And the r-adaptivity refinement was also implemented.[Maenghyo Cho and Seongki Jun (2004)].

But, in our previous study, B-spline surface functions were used to generate the surfaces. Of course, B-spline surfaces provide more control flexibility than other surface equations such as Bezier equations. But B-spline surfaces are still polynomial functions so it's impossible to represent the quadric surfaces exactly. On the other hands, NURBS surface can represent the quadric surfaces exactly in a mathematical point of view. And the definition of NURBS surface function is from ratios of polynomials so permits much better control over the curvature of surfaces than polynomial alone. NURBS surface function also gives much more flexibility than B-spline functions by introducing weighting factors. So it is known that the NURBS surface equation is the most general form of surface equations. This is the reason why the most current commercial CAD systems adopt the NURBS technology to generate the surfaces. Therefore, in this study, NURBS surface equations are employed instead of B-spline surface equations and all necessary geometric quantities are calculated directly from them.

Other approaches integrating finite element with B-spline or NURBS equations and utilizing the advantages of them can be found lately in a variety of fields. Xiang.Jiawei *et al*. (2008) suggested flat shell element using B-spline wavelet which has high performance in shell structure analysis especially for folded plate structures. The generalization of a NURBS based parametric mesh-free method was also studied by Amit Shaw *et al.* (2008).

The outline of this paper is as follows. First, we review the definition of NURBS

surface and its properties are briefly summarized. And then, the procedure and advantages of our approach for the computation of geometric quantities for the shell finite element analysis will be described, followed by the NURBS surface generation and data exchange, which is related to the implementation of the linkage framework of geometric modeling and geometrically exact shell finite element. Finally, several numerical examples are given to assess the accuracy of the numerical performances and the capability of our proposed linkage framework to handle the various kinds of shell surfaces represented by the NURBS equation. The NURBS surface was generated by interpolating a given set of data points and analytically exact NURBS surface as well as trimmed NURBS surface.

2 NURBS Surface Representation

Over the past several decades, many curves and surfaces representation forms have been proposed. Presently, the most popular mathematical forms are B-splines and NURBS(non-uniform rational B-splines). Especially, the NURBS offers a unified mathematical form not only for the representation of free-form surfaces but also for the precise representation of close-form surfaces such as lines, conics, quadrics and surfaces of revolution. Further, the NURBS offers flexible surface modeling by allowing many degrees of freedom through the modification control points and weights. Therefore, the NURBS has been an IGES standard since 1983, and many commercial CAD systems are based on the NURBS representation. The NURBS representation is adopted to link the developed geometrically exact shell element to the geometric modeling in CAD systems in our study. The definition and important properties of NURBS surfaces are briefly outlined here. The detailed contents can be found in references [Les Piegl, Wayne Tiller (1997), G. Farin (1993), C. De Boor (1972)].

2.1 Definition of NURBS Surfaces

The NURBS surface $S(u,v)$ of degree (p,q) is defined as

$$S(u,v) = \frac{\sum_{i=0}^{n}\sum_{j=0}^{m} N_{i,p}(u)N_{j,q}(v)w_{i,j}\mathbf{P}_{i,j}}{\sum_{i=0}^{n}\sum_{j=0}^{m} N_{i,p}(u)N_{j,q}(v)w_{i,j}} \qquad 0 \le u,v \le 1 \tag{1}$$

where the $\mathbf{P}_{i,j}$ is a bidirectional control net, and the $w_{i,j}$ are weights. And the ith B-spline basis function of degree p, denoted by $N_{i,p}(u)$, is defined by the recurrence formula as follows.

$$N_{i,0}(u) = \begin{cases} 1 & \text{if } u_i \le u < u_{i+1} \\ 0 & \text{if otherwise} \end{cases} \tag{2}$$

$$N_{i,p}(u) = \frac{u-u_i}{u_{i+p}-u_i}N_{i,p-1}(u) \qquad + \frac{u_{i+p+1}-u}{u_{i+p+1}-u_{i+1}}N_{i+1,p-1}(u) \tag{3}$$

where $N_{i,p}$ and $N_{j,q}$ are the non-rational B-spline basis functions defined on the knot vectors

$$U = \{0,\ldots,0,u_{p+1},\ldots,u_{r-p-1},1,\ldots 1\} \tag{4a}$$

$$V = \{0,\ldots,0,v_{q+1},\ldots,v_{r-q-1},1,\ldots,1\} \tag{4b}$$

The degree(p or q), the number of knots(r or s) of the surface and the number of control points(n or m) are related by the formula: $r = n+p+1$, $s = m+q+1$. The surface defined by Eq.(1) becomes a B-spline surface if all weights are equal. If the weights are not equal and there are no interior knots, the surface defined by Eq.(1) becomes a rational Bezier surface: that is, the NURBS surface equation is a general form that includes the B-spline and Bezier surface equations.

2.2 Computation of Geometric Quantities for the Shell FEA from NURBS Equation

Some geometric quantities of the shell surface, which are required in implementing the geometrically exact shell element for the shell finite element analysis, are as follows: covariant base vectors $\vec{a}_\alpha$, normal vector $\vec{a}_3$, covariant metric tensor $a_{\alpha\beta}$, surface curvature tensor $b_{\alpha\beta}$ and 2^{nd} kind of Christtoffel symbols $\Gamma^\gamma_{\alpha\beta}$ etc. If we know the exact analytical expression for the position vector $\vec{r}(\theta^1,\theta^2)$ of the surface, then all the geometric quantities which are mentioned above can be easily calculated from the position vector. But it is almost impossible to obtain the position vector of the general surface except for some simple surfaces such as cylindrical surfaces or spherical surfaces and so on. Otherwise, the NURBS equation can represent the general surfaces, and we can extract the necessary geometric quantities directly from the NURBS equation and compute the values of the metric tensor or curvature tensor because the NURBS surface can be differentiated $p-k(q-k)$ times in the u , v directions, as mentioned in the previous section. For this reason, we employ the NURBS equation for the general shell surface analysis and this property of the NURBS surface is one of the major advantages. Especially, the derivatives of the surface at a specific point (actually, at gauss points) are needed to generate for the geometrically exact shell element because the computation of surface curvature tensor $b_{\alpha\beta}$, metric tesnor $a_{\alpha\beta}$ and the 2^{nd} kind of Christtoffel symbols $\Gamma^\gamma_{\alpha\beta}$ requires the base vectors $\vec{a}_\alpha$ and $\vec{a}_3$ as shown in Fig.1(a). The surface curvature tensor and 2^{nd} kind of Christtoffel symbols can be calculated from the following relationships

$$b_{\alpha\beta} = \vec{a}_3 \cdot \vec{a}_{\beta,\alpha}$$

$$\Gamma^{\gamma}_{\alpha\beta} = a^{\gamma\lambda}\vec{a}_{\lambda}\cdot\vec{a}_{\alpha,\beta} \tag{5}$$

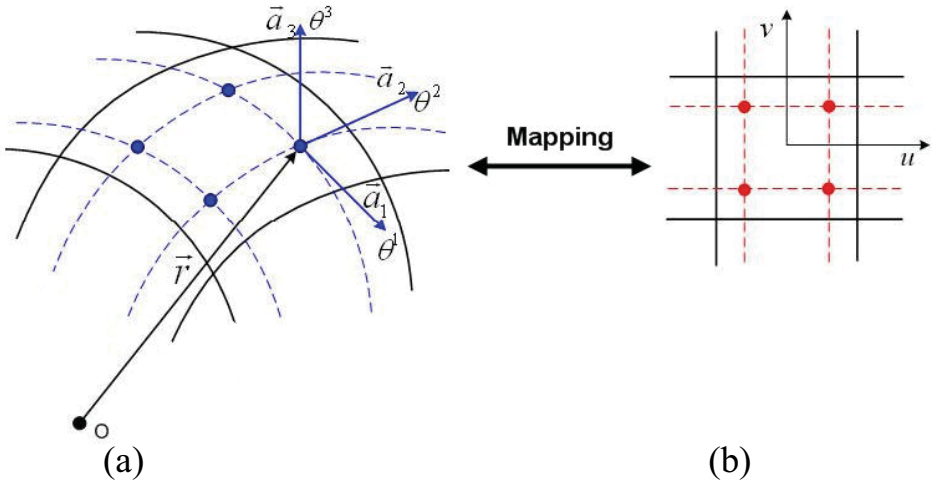

Figure 1: (a) Configuration of shell surface (b) Parametric domain of NURBS surface

If analytical closed form of the position vector is available, for example, in the case of a cylindrical surface, $\vec{r}(\theta^1,\theta^2) = r\cos(\theta^1)\vec{e}_x + r\sin(\theta^1)\vec{e}_y + \theta^2\vec{e}_z$, the analytical calculations of the geometric quantities become straightforward. The base vectors $\vec{a}_\alpha$ can be computed by the following expression.

$$\vec{a}_\alpha = \frac{\partial\vec{r}}{\partial\theta^\alpha}, (\alpha = 1,2) \quad \vec{a}_3 = \frac{\vec{a}_1\times\vec{a}_2}{|\vec{a}_1\times\vec{a}_2|} \tag{6}$$

And all other necessary geometric quantities can be obtained from the base vectors and their first derivatives. But, when the analytical closed form of position vector is not known, the derivatives of position vector cannot be calculated directly from Eq.(6).

However, if the surface is represented by the NURBS equation as shown Eq.(1), the derivatives of the surface $S(u,v)$ can be computed assuming that (u,v) is fixed. There are two partial derivatives: one with respect to u and one with respect to v. Generally, all partial derivatives of the surface $S(u,v)$ up to and including order d are computed as,

$$\frac{\partial^{k+l}}{\partial u^k\partial v^l}S(u,v) \quad 0\le k+l\le d \tag{7}$$

where k and l represent the orders of the derivative of $S(u,v)$ with respect to u and v.

In the more detailed form, the derivatives of the surface can be written as

$$\begin{aligned}\frac{\partial S(u,v)}{\partial u} &= \left(\sum_{i=0}^{n}\sum_{j=0}^{m}\frac{\partial N_{i,p}(u)}{\partial u}N_{j.q}(v)w_{i.j}P_{i,j}\right)\frac{\left(\sum_{i=0}^{n}\sum_{j=0}^{m}N_{i,p}(u)N_{j,q}(v)w_{i,j}\right)}{\left(\sum_{i=0}^{n}\sum_{j=0}^{m}N_{i,p}(u)N_{j,q}(v)w_{i,j}\right)^2} \\ &\quad - \left(\sum_{i=0}^{n}\sum_{j=0}^{m}N_{i,p}(u)N_{j.q}(v)w_{i.j}P_{i,j}\right)\frac{\left(\sum_{i=0}^{n}\sum_{j=0}^{m}\frac{\partial N_{i,p}(u)}{\partial u}N_{j,q}(v)w_{i,j}\right)}{\left(\sum_{i=0}^{n}\sum_{j=0}^{m}N_{i,p}(u)N_{j,q}(v)w_{i,j}\right)^2}\end{aligned} \tag{8a}$$

$$\begin{aligned}\frac{\partial S(u,v)}{\partial v} &= \left(\sum_{i=0}^{n}\sum_{j=0}^{m}N_{i,p}(u)\frac{\partial N_{j.q}(v)}{\partial v}w_{i.j}P_{i,j}\right)\frac{\left(\sum_{i=0}^{n}\sum_{j=0}^{m}N_{i,p}(u)N_{j,q}(v)w_{i,j}\right)}{\left(\sum_{i=0}^{n}\sum_{j=0}^{m}N_{i,p}(u)N_{j,q}(v)w_{i,j}\right)^2} \\ &\quad - \left(\sum_{i=0}^{n}\sum_{j=0}^{m}N_{i,p}(u)N_{j.q}(v)w_{i.j}P_{i,j}\right)\frac{\left(\sum_{i=0}^{n}\sum_{j=0}^{m}N_{i,p}(u)\frac{\partial N_{j,q}(v)}{\partial v}w_{i,j}\right)}{\left(\sum_{i=0}^{n}\sum_{j=0}^{m}N_{i,p}(u)N_{j,q}(v)w_{i,j}\right)^2}\end{aligned} \tag{8b}$$

As shown in Eq.(8a), we need to obtain the derivatives of the B-spline basis function. Let $N_{i,p}^{(k)}$ denote the kth derivative of the B-spline basis function $N_{i,p}^{(}u)$, then,

$$N_{i,p}^{(k)}(u) = p\left(\frac{N_{i,p-1}^{(k-1)}}{u_{i+p}-u_i} - \frac{N_{i+1,p-1}^{(k-1)}}{u_{i+p+1}-u_{i+1}}\right) \tag{9}$$

$N_{j,q}^{(l)}$ is also represented in the same manner.

Therefore, the derivatives of the NURBS surface in the u,v direction can be computed if the corresponding (u,v) parameter values are given. Because there is one-to-one mapping relationship between a specific point on the surface in the Cartesian coordinates and a point in the (u,v) parametric domain as shown Fig.1, the basis vectors needed for the geometrically exact shell finite element analysis can be computed directly from the NURBS equation if we specify the u and v values. Fig.2

shows the computed results of the basis vector at the Gauss points in each element.

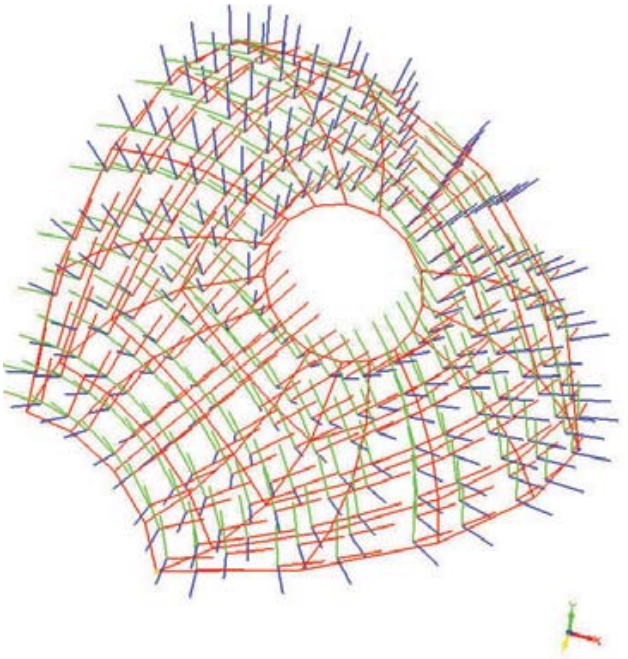

Figure 2: The basis vector at gauss points (red line: u direction, green line: v direction, blue line: normal direction)

The geometric errors can be reduced dramatically in this approach. Generally, in the case of a flat facet element, the necessary geometric quantities at Gauss points are computed by interpolating the nodal values (Fig.3). It is very difficult to avoid the inherent geometrical errors, but, in the present approach, all geometric quantities can be computed directly at Gauss points from the NURBS equations without interpolation. As shown in Fig.4, there is a difference between the normal vector which is computed by interpolating nodal values and the normal vector which is computed directly from the NURBS equation. Therefore, we can expect a very small geometric error even though a coarse mesh is used for the analysis.

3 Linkage Framework : The NURBS Surface Generation and Data Exchange

The present study aims at the development and implementation of the linkage framework between the geometrically exact shell finite element and the NURBS

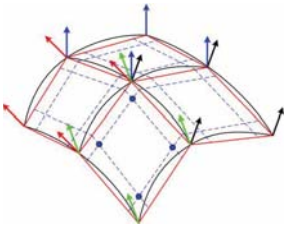

(a) Normal vectors of each elements

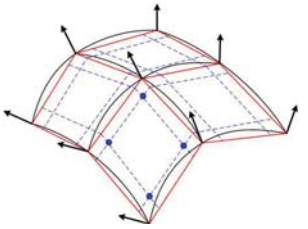

(b) Normal vectors at nodes

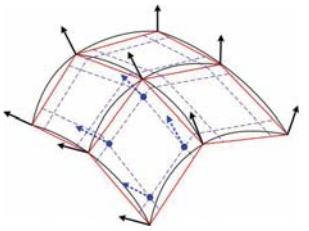

(c) Normal vectors at gauss points

Figure 3: Normal vectors of flat facet element

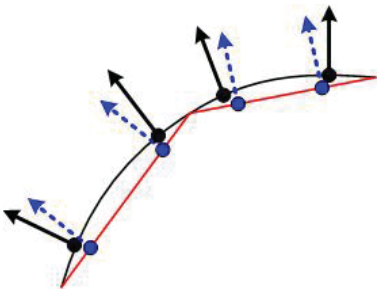

Figure 4: Difference between the directly computed normal vectors and normal vectors of flat facet shell element

surface representation. Our developed program can import two kinds of data for the NURBS surface generation: one is the surface scanning data and the other is the geometric data which are modeled and saved in IGES file format in the CAD systems.

After the surface scanning data are imported, NURBS surface is generated by fitting a given set of data points. Generally, there are two types of fitting, interpolation and approximation. In the case of interpolation, a surface satisfying the given data precisely is constructed, but, in approximation, surfaces do not necessarily satisfy the given data precisely, but only approximately. In some actual applications, such as the generation of point data by use of a coordinate measurement device or digitizing scanner, a large number of points can be generated. So, we often need to make the surface with a given set of data points by the interpolation or approximation methodologies.

In NURBS technology, the desirable NURBS surface can be generated by appropriate fitting, interpolation or approximation. Usually, the input of the fitting problem consists of geometric data, such as points and derivatives, and the output consists of a NURBS surface, that is, the control points, knots and weights. The degree (p,q) for surfaces also must be specified in advance or selected automatically by the algorithm. Our developed program supports these two types of fitting method, but this study focuses on the interpolation methodology. Fig.5 shows the NURBS surfaces generated by interpolating surface geometry data points. The methods for generating the interpolated NURBS surfaces can be classified into three types according to the type of parameterization, namely, *uniform*, *chord length* and *centripetal* parameterizations. When the knot spacing is uniform, that is, the difference between successive knots is the same regardless of the actual length of the curve segment in the u, v direction on the surfaces, we call it *uniform* parameterization; this method works best for an evenly-spaced surface of u, v rows and columns. With *chord length* parameterization, the difference between successive knot values is related to the actual length of each segment, that is, the knot values are not equal. When the surface spacing is not uniform, this would be an adequate method. With the *centripetal* parameterization, the knot spacing is related to the square root of the length of each curve segment. In some cases, this may make smoother objects. On the surfaces of very unevenly spaced control points, the *centripetal* parameterization may give slightly better results than the *chord length*. In Fig.6, the point spacing is un-evenly distributed. The smoother curve is defined by using centripetal knot spacing. In the later section, the difference of analysis results according to the parameterization methods will be shown.

Generally, most fitting algorithm can be classified into two categories: global or local. In this study, the interpolated NURBS surface is generated by using the

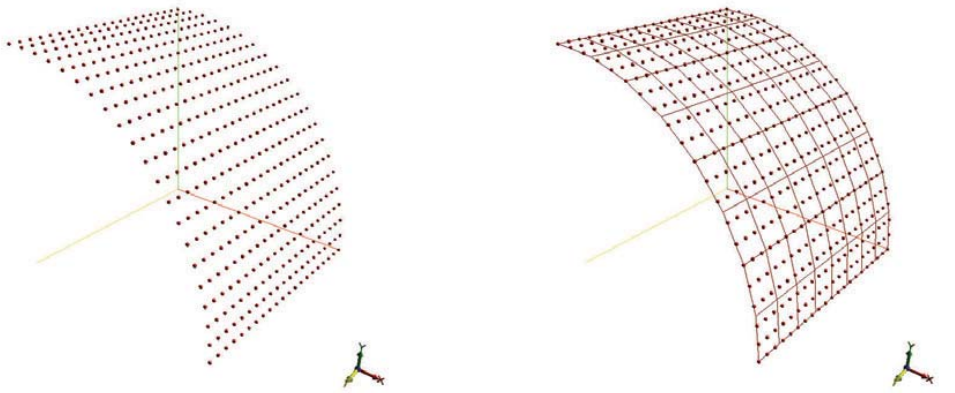

Figure 5: NURBS surface generation by interpolating geometry data points

Figure 6: Difference between *uniform* (unfair) and *centripetal* (smooth) knot spacing

global algorithm. If a given set of data points $\{Q_{k,l}\}$, $k = 0,\ldots,n$ and $l = 0,\ldots,m$, and we want to construct a non-rational (p,q)th–degree B-spline surface interpolating these points, the control points of the desired surface can be obtained from the following relation.

$$Q_{k,l} = S(\bar{u}_k, \bar{v}_l) = \sum_{i=0}^{n} \sum_{j=0}^{m} N_{i,p}(\bar{u}_k) N_{j,q}(\bar{v}_l) P_{i,j} \tag{10}$$

First, reasonable values for $(\bar{u}_k, \bar{v}_l)$ and the knot vectors U and V must be computed. The selection of the coordinate value of the surface parameter $(\bar{u}_k, \bar{v}_l)$ affects the shape and parameterization of the surface. As mentioned above, there are three common methods of choosing the parameter coordinate values $(\bar{u}_k, \bar{v}_l)$. The first

one is the *uniform* method. But this method is not recommended because it can produce undesirable surfaces when the data are unevenly spaced. Here the calculation of $\bar{u}_k$ is only explained for convenience. the $\bar{v}_l$ is also computed in the same manner.

$$\bar{u}_0 = 0, \quad \bar{u}_n = 1, \quad \bar{u}_k = \frac{k}{n} \quad k = 1, \ldots, n-1 \tag{11}$$

The second one is the *chord length* method. This is the most widely used method, appropriate for most cases. It gives a good parameterization to the curve or surface. The total chord length (d) is

$$d = \sum_{k=1}^{n} |Q_k - Q_{k-1}| \tag{12}$$

And then, we can calculate $\bar{u}_k$ as follows

$$\begin{aligned} &\bar{u}_0 = 0 \quad \bar{u}_n = 1 \\ &\bar{u}_k = \bar{u}_{k-1} + \frac{|Q_k - Q_{k-1}|}{d} \quad k = 1, \ldots, n-1 \end{aligned} \tag{13}$$

The third one is the *centripetal* method. The total chord length is given as

$$d = \sum_{k=1}^{n} \sqrt{|Q_k - Q_{k-1}|} \tag{14}$$

And the corresponding $\bar{u}_k$ is obtained from the following equations

$$\begin{aligned} &\bar{u}_0 = 0 \quad \bar{u}_n = 1 \\ &\bar{u}_k = \bar{u}_{k-1} + \frac{\sqrt{|Q_k - Q_{k-1}|}}{d} \quad k = 1, \ldots, n-1 \end{aligned} \tag{15}$$

This is a new method [Lee, E.T.Y.(1989)] which gives better results than the *chord length* method, when the data points are very unevenly spaced or take very sharp turns.

From these calculated $\bar{u}_k$ values, we can compute the knots by using the average method. The knots obtained with this averaging technique reflect the distribution of the $\bar{u}_k$, properly.

$$\begin{aligned} &u_0 = \ldots = u_p = 0 \quad u_{m-p} = \ldots = u_m = 1 \\ &u_{j+p} = \frac{1}{p} \sum_{i=j}^{j+p+1} \bar{u}_i \quad j = 1, \ldots, n-p \end{aligned} \tag{16}$$

Moreover Eq.(16) combined with Eq.(13) and Eq.(15) gives a totally positive and banded system with a bandwith of less than p, q, that is,

$$N_{i,p}(\bar{u}_k) = 0 \quad \text{if } |i-k| \geq p,$$
$$N_{j,q}(\bar{v}_k) = 0 \quad \text{if } |j-l| \geq q$$

[De Boor, C.(1978)].

Therefore it can be easily solved by a simple linear solver.

The other way to generate the NURBS surface is to obtain the necessary geometric data from the surfaces which is modeled in the CAD systems. The most current CAD systems generate surfaces based on the NURBS representation. Therefore, this function is very useful because the geometric data from the CAD systems can be used directly in the analysis routine without any other manipulations and can provide an integrated design of modeling and analysis interactively.

At present, our developed program imports the general surfaces including the trimmed surfaces and it generates the NURBS surfaces from the imported surface geometric data. Data between a CAD software and developed program are exchanged via the IGES file format, which serves as a neutral data format for transference of design between dissimilar CAD systems. Some examples are illustrated in Fig.7.

After the surface geometric data are imported and converted into the NURBS surface, discretized elements have to be prepared for the analysis. To do so, the mesh generation process is necessary. Because quadrilateral four and nine node shell elements are used in our current study, the structural rectangular mesh generation is required. When the NURBS surfaces are generated by interpolation with the given data points and by the import of an IGES format file of the general surfaces, the mesh is generated automatically by the embedded algorithm. But, in the case of trimmed surfaces, the procedure is slightly different. It was not easy to manipulate a trimmed surface in our previous work using the B-spline surface equations. Because the B-spline surface patch is not allowed to have a hole in the middle of it. However the NURBS surfaces can be trimmed with segments that carve holes out of the inside. For example, a surface with a hole in it can be represent by B-spline surface or NURBS surface. As shown in Fig.8, the trimmed surface represented by B-spine surface functions requires several patches but the trimmed surface represented by NURB surface functions is trimmed by two arcs. Therefore, the NURBS surface makes modeling much faster and easier for a trimmed surface and surfaces with a hole can be dealt more easily in this study by utilizing the NURBS surface instead of B-spline surface.

The trimmed surface is defined by two items: the information of the surface itself and the information of its trimming curves of the surface. If any parametric curve

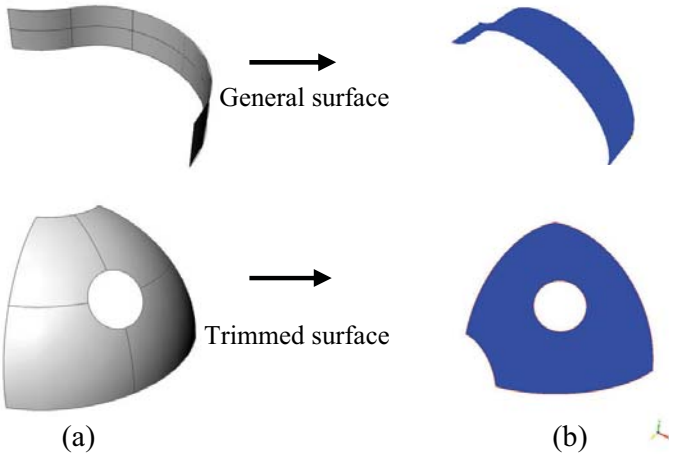

Figure 7: (a) Modeling in the CAD system (b) Visualization of imported surface data (data transformation between two of them in IGES file format)

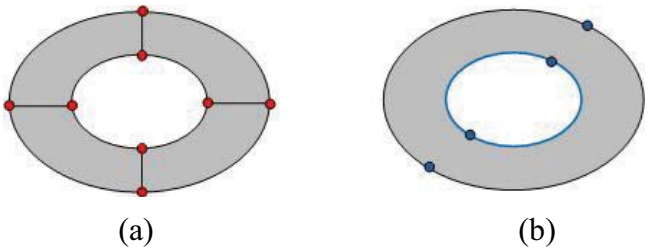

Figure 8: Trimmed surfaces: (a) Representation using B-spline surface patches (b) Representation using NURBS surface equation

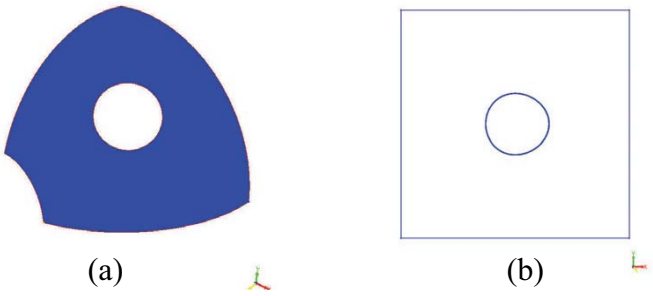

Figure 9: A trimmed surface: (a) 3-D model space and (b) 2-D parameter space

$(u(t), v(t))$ is created in the domain of a surface $S(u, v)$, it will be mapped to a curve on the surfaces. Fig.9 illustrates this concept and the fact that the shape of the 3D curve on the surface is a distorted version of the curve on the parametric domain.

The mesh generation is performed in the (u, v) parametric domain. First, inner and outer trimming curves of the trimmed surface are extracted as shown in Fig.10(a), and the parametric domain is divided appropriately in advance for the structural mesh generation, as shown in Fig.10(b), And then, the mesh is generated in each sub-region of the entire parametric domain and the mesh is refined in this parametric domain, if necessary (Fig.10(d)).

Because there is a one-to-one mapping relationship between the 2-D (u, v) parametric domain and the 3-D model domain, this mesh data can be mapped to the original trimmed surface in the 3-D model space. Fig. 11 illustrates this.

These quadrilateral elements are used in the finite element analysis routine. All geometric quantities actually are computed at the Gauss points by using the NURBS equation. Accordingly, the u, v values of Gauss points of each element are also calculated in the 2-D parametric domain and then mapped to the original trimmed surface in the 3-D model domain. These u, v values of the Gauss points act as the input data to the function that computes the geometric quantities from the NURBS equations.

4 Numerical Examples

In this section, well-known benchmark shell problems are considered in order to test the performance of the present shell element with the NURBS representation. The present results are compared with those of the analytical closed forms previously reported. In this section, the analysis results are classified into three categories according to the type of NURBS surfaces: the NURBS surfaces generated by interpolation, the exact NURBS surface which is identical to the analytical closed form surface and the trimmed NURBS surface. The assumed nine-node shell element with bubble displacement functions, which was developed in our previous work is used in all problems.

4.1 Case 1: The NURBS Surface Generated by Interpolation

There are three kinds of parameterization methods for generating interpolated NURBS surfaces: *uniform*, *chord length* and *centripetal*. Here, the NURBS surfaces are generated by using each parameterization method, and the analysis results of each case are compared to one another. The convergence rates and trends of the parameterization methods are slightly different from one another depending on the problems.

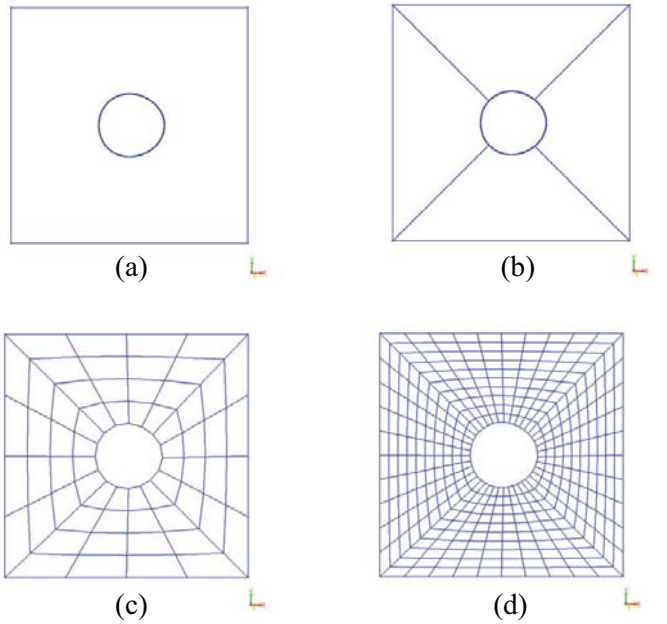

Figure 10: Structural quadrilateral mesh generation and mesh refinement

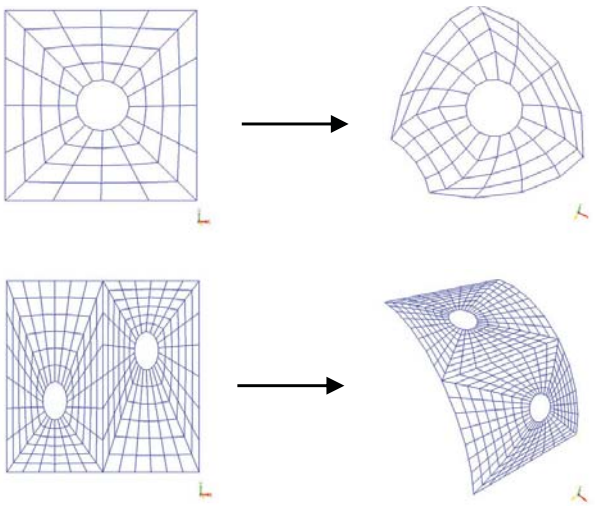

(a) (u,v) parametric domain (b) 3-D model domain

Figure 11: The mapping relationship between parametric and model domain

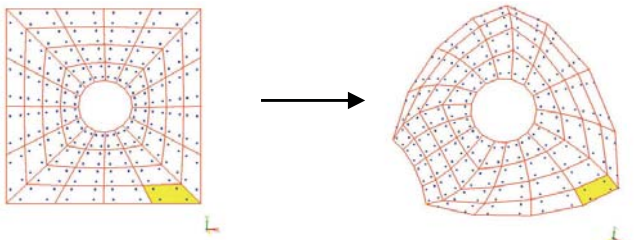

(a) (b)

Figure 12: Mapping of gauss points from 2-D parametric domain to 3-D model domain (in case of 4-node quadrilateral element)

4.1.1 Pinched Cylinder with Rigid Diaphram

A pinched cylinder with diaphragmed ends is considered. Radial loads of $F = 1.0$ is applied at the mid-section of the cylinder. The length $L = 600$, radius $R = 300$, thickness $h = 3.0$, Young's modulus $E = 3 \times 10^6$ and Possion ratio $\nu = 0.3$. The analytical displacement is 1.8248×10^{-5}. This is known as one of the benchmark problems of bending dominant behavior in the thin limit.

The solution obtained by the present element is greater than the Flugge's analytical solution because the shell theory used by Flugge does not include transverse shear deformation unlike the present formulation. Thus, the numerical results of the present shell element are also compared with another convergent reference solution provided by NASTRAN QUAD8 element which allows transverse shear deformation. The transverse deflection is equal to 1.8541×10^{-5}. Fig.14(a) shows the convergence rates of displacement of the exact surface and the NURBS surfaces, which are generated using the *uniform* parameterization method. And Fig.14(b) and (c) indicate the convergence of the NURBS surface, which is generated by using the *centripetal* and *chord length* parameterization respectively. In this example, the convergence rate of the NURBS surface generated by using *uniform* parameterization is better than that of the NURBS surfaces generated by using the *chord length* or *centripetal* parameterization. In this cylindrical surface problem, the knot spacing is uniform in each u, v direction. Therefore, it is considered that *uniform* parameterization method works better than the others. In Fig.15, the result of the displacement convergence of the present method is compared with the result using the MITC8 element. The present geometrically exact shell element integrated with the NURBS equation works very well even for a coarse mesh configuration.

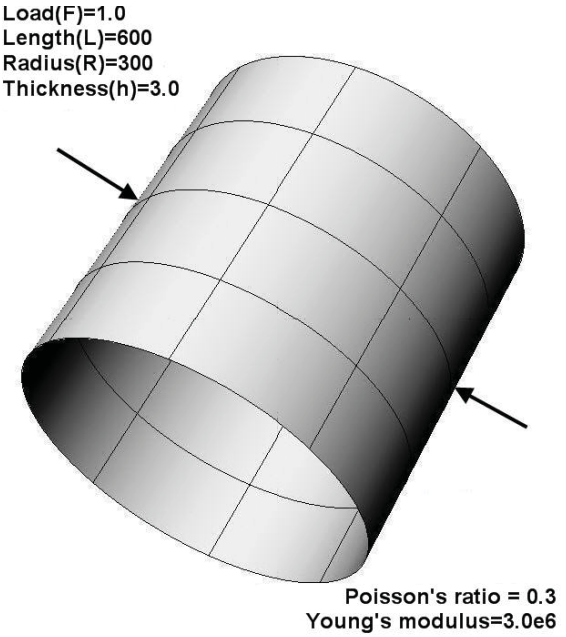

Figure 13: Pinched cylinder with rigid diaphragm end condition

4.1.2 Pinched Hemispherical Shell with 18° *Cut-out*

A hemispherical shell, with an 18° cutout at the apex, subjected to alternating loads, is analyzed. The geometry and material properties used are as follows: the radius of the hemi-sphere $R = 10$, the thickness $h = 0.04$, Young's modulus $E = 6.258 \times 10^7$ and Poisson's ratio $\nu = 0.3$. The edge of the shell is free. The applied loads have a magnitude $F = 2$and define two pairs of diametrically opposite loads alternating in sign at 90°. The convergence of the radial displacement under applied loads is shown in Fig.16. The result of this problem is better when the NURBS surface is generated by using the *chord length* and the *centripetal* parameterization methods than by using the *uniform* method. The *chord length* and *centripetal* methods give similar results as shown in Fig.17(b), and 17(c). In Fig.18, the rate of convergence of the present result is compared with those of the solutions previous published, such as that obtained from the used of the S08 shell element of Stander et al. [N.Stander, A. Matzenmiller, E. Ramm(1989)] with the uniformly reduced and well-established Bathe-Dvorkin element(MITC8) [K.Y. Bathe, E.M. Dvorkin(1986)]. Our result shows outstanding performance despite of the coarse mesh and very rapid convergence compared to results obtained with use of other elements.

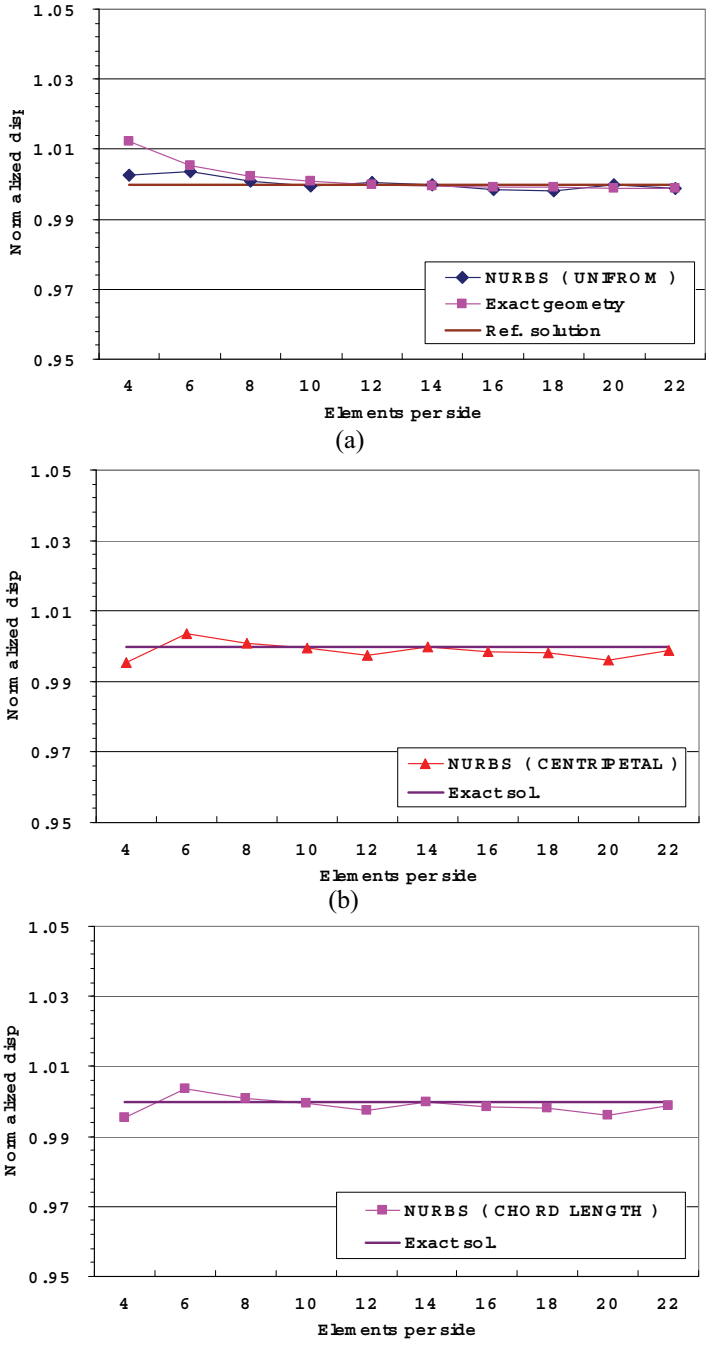

Figure 14: Convergence of the normalized radial displacement (the displacement normalized by 1.8541×10^{-5})

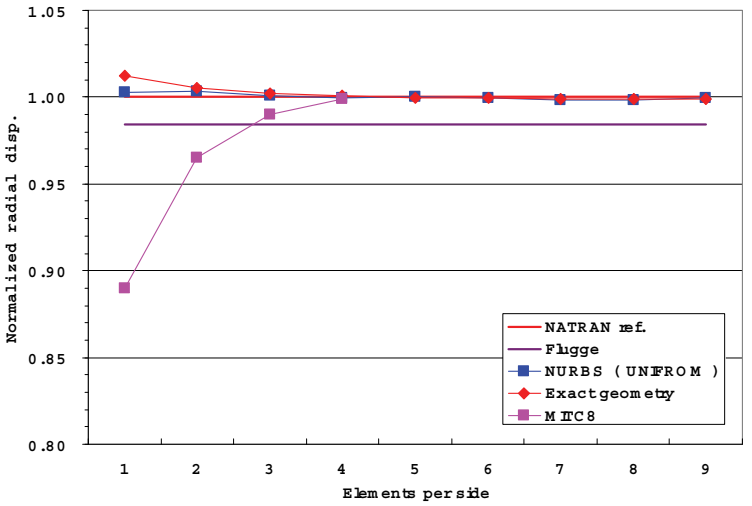

Figure 15: Comparison of the convergence

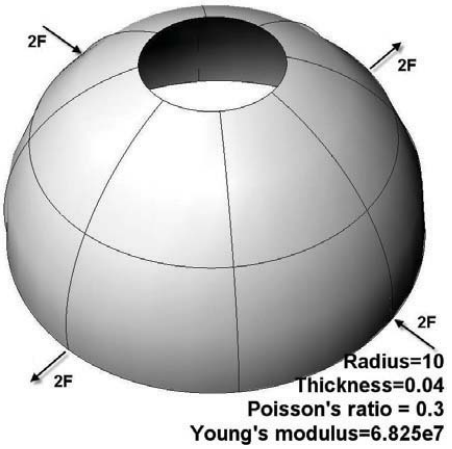

Figure 16: Pinched hemispherical problem configuration

4.1.3 Mexican Hat Problem

This benchmark problem can be characterized by a rapid change of curvature to assess shell element performance.

Fig. 19 shows the configuration of a Mexican hat problem. The geometry and material properties: Thickness $h = 0.04$, Young's modulus $E = 3.0 \times 10^7$, Possion's ratio $\nu = 0.3$.

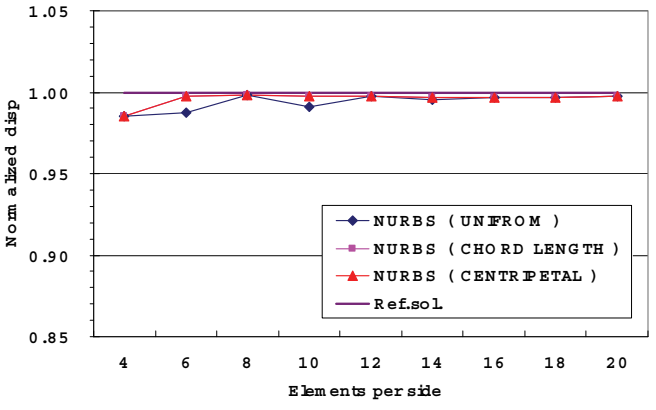

(a)

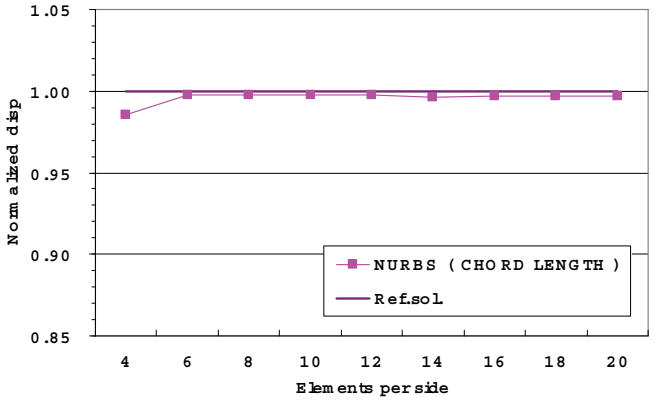

(b)

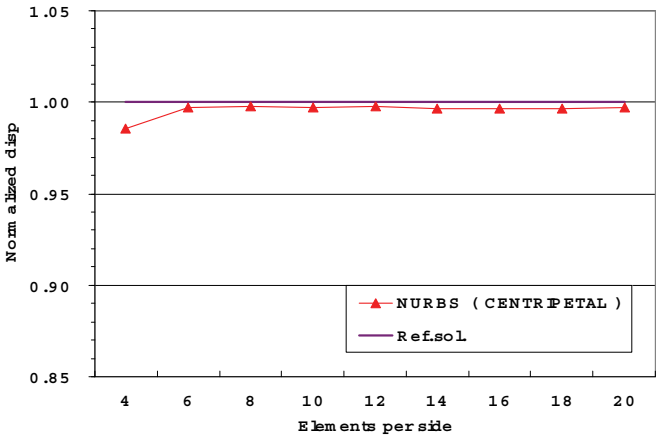

(c)

Figure 17: Convergence of the normalized radial displacement (displacement normalized by 0.094)

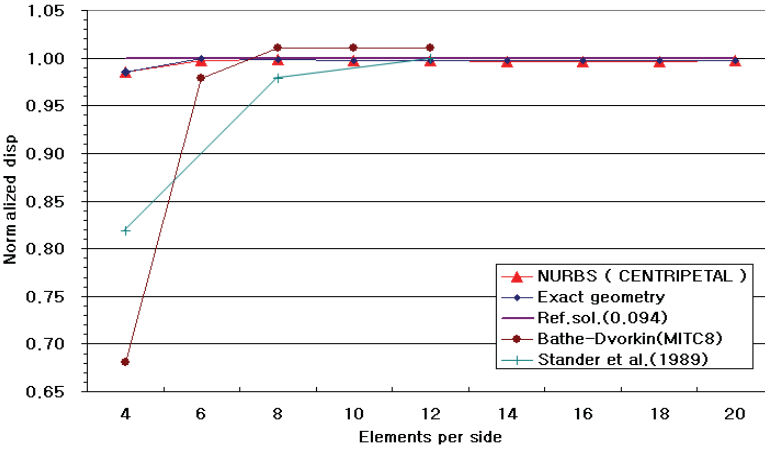

Figure 18: Comparison of the convergence

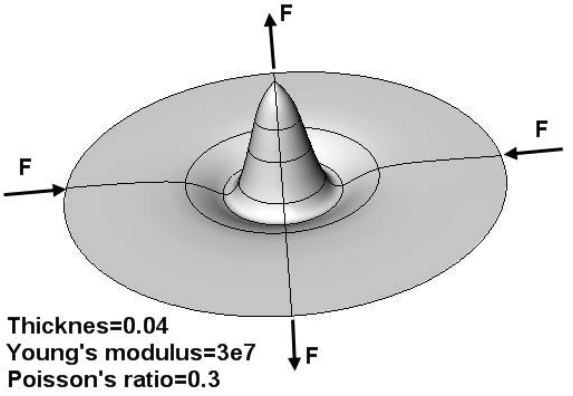

Figure 19: Mexican hat problem configuration

The parameterized surface of the Mexican hat can be expressed in the analytical closed form.

$$\vec{r}(\theta^1,\theta^2) = r\cos(\theta^1)\vec{e}_x + r\sin(\theta^1)\vec{e}_y + \theta^2\vec{e}_z \tag{17a}$$

where,

$$x(\theta^1,\theta^2) = \theta^1\cos(\theta^2), \quad y(\theta^1,\theta^2) = \theta^1\sin(\theta^2)$$

$$z(\theta^1,\theta^2) = \left(\frac{\sigma^2-(\theta^1)^2}{\sigma^4}\right)\exp\left(\frac{-(\theta^1)^2}{2\sigma^2}\right) \tag{17b}$$

The curvature changes according to the value of parameter σ. In this problem, the value of σ is set equal to 1. The result is better when the NURBS surface is generated by using the *centripetal* parameterization than generated by using the *uniform* or the *chord-length* parameterizations, as depicted in Fig.20(b). Generally, a smoother surface is defined by using the *centripetal* parameterization when the control points are very unevenly spaced.

4.2 Case 2 : Analytically Exact NURBS Surface

The NURBS equation can exactly represent the quadratic cylindrical, spherical, and conical surfaces etc. This property, especially, is very useful with respect to geometry as well as analysis, because most current engineering surface designs are a combination of quadric surfaces.

4.2.1 Pinched Cylinder with Rigid Diaphram

The geometry and material properties of this example are the same as those given in section **5.1**.

The analytical closed form of the cylinder is written as

$$\vec{r}(\theta^1,\theta^2) = r\cos(\theta^1)\vec{e}_x + r\sin(\theta^1)\vec{e}_y + \theta^2\vec{e}_z \tag{18}$$

where $x(\theta^1,\theta^2) = r\cos(\theta^1)$, $y(\theta^1,\theta^2) = r\sin(\theta^1)$ and $z(\theta^1,\theta^2) = \theta^2$. In Fig.22, "Exact geometry" means that all geometric quantities such as surface metric, curvature tensor and Christoffel symbols are computed from Eq.(18). And "Exact NURBS" implies that the cylindrical surface is generated with the configuration given by Fig.21. Actually, this surface is modeled in the CAD system and saved in an IGES format file. Our developed program imports this file and performs the analysis. As shown in Fig. 22, the two results are almost the same.

4.2.2 Pinched Hemispherical Shell with 18° *Cut-out*

The geometry and material properties of this example are the same as the one shown in section **5.1**. The values of control points and corresponding weights are specified appropriately to represent the exact NURBS surface.

The analytical closed form of the hemispherical surface is expressed by

$$\vec{r}(\theta^1,\theta^2) = r\cos(\theta^1)\vec{e}_x + r\sin(\theta^1)\vec{e}_y + \theta^2\vec{e}_z \tag{19}$$

where,

$$x(\theta^1,\theta^2) = r\sin(\theta^1)\cos(\theta^2)$$

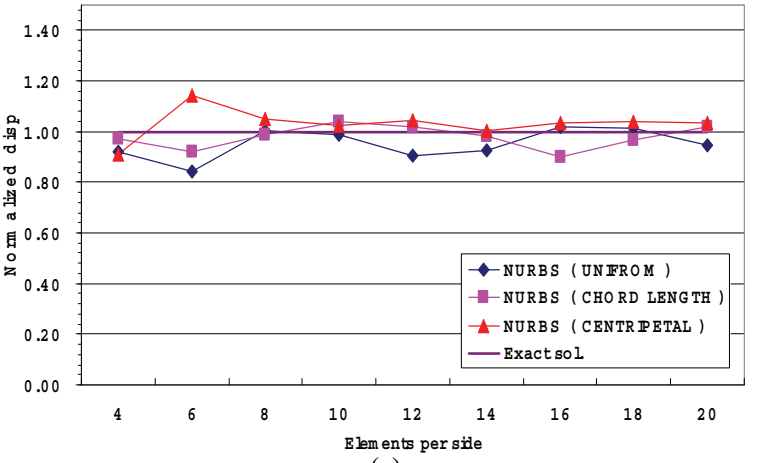

(a)

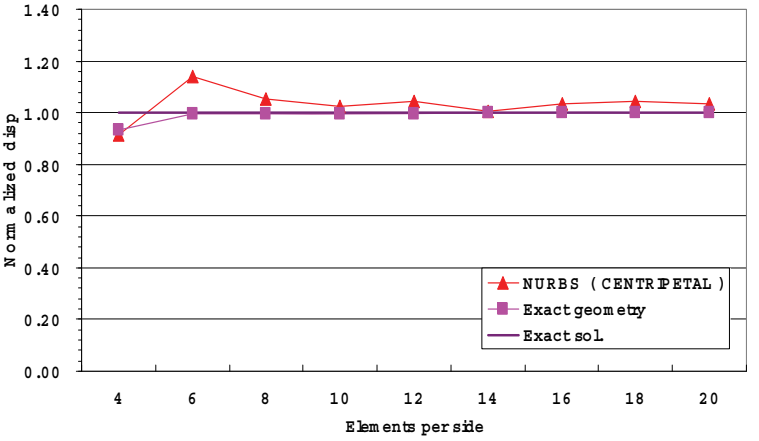

(b)

Figure 20: Convergence of normalized radial displacement

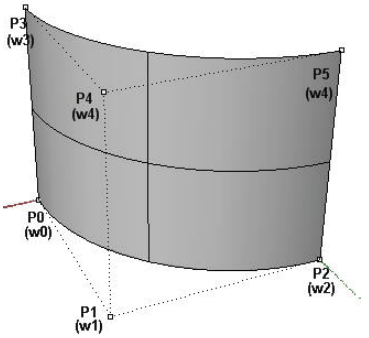

$\mathbf{P}_0 = (300,0,0)$ $\quad \mathbf{w}_0 = 1$

$\mathbf{P}_1 = (300,300,0)$ $\quad \mathbf{w}_1 = \sqrt{2}/2$

$\mathbf{P}_2 = (0,300,0)$ $\quad \mathbf{w}_2 = 1$

$\mathbf{P}_3 = (300,0,300)$ $\quad \mathbf{w}_3 = 1$

$\mathbf{P}_4 = (300,300,300)$ $\quad \mathbf{w}_4 = \sqrt{2}/2$

$\mathbf{P}_5 = (0,300,300)$ $\quad \mathbf{w}_5 = 1$

Figure 21: The values of control points and weights for the exact NURBS surface

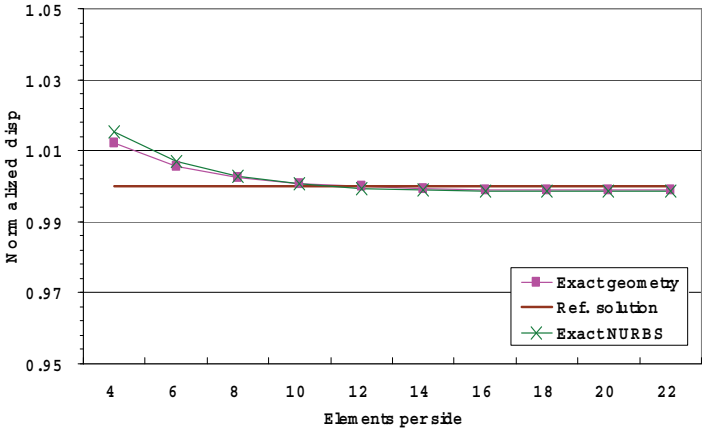

Figure 22: Convergence of normalized radial displacement

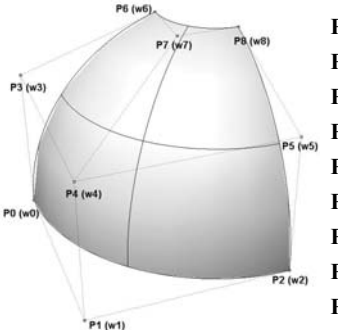

$$\mathbf{P}_0 = (10,0,0) \quad \mathbf{w}_0 = 1$$
$$\mathbf{P}_1 = (10,10,0) \quad \mathbf{w}_1 = \sqrt{2}/2$$
$$\mathbf{P}_2 = (0,10,0) \quad \mathbf{w}_2 = 1$$
$$\mathbf{P}_3 = (10,0,7.265) \quad \mathbf{w}_3 = 0.809017$$
$$\mathbf{P}_4 = (10,10,7.265) \quad \mathbf{w}_4 = 0.572061$$
$$\mathbf{P}_5 = (0,10,7.265) \quad \mathbf{w}_5 = 0.809017$$
$$\mathbf{P}_6 = (3.090,0,9.511) \quad \mathbf{w}_6 = 1$$
$$\mathbf{P}_7 = (3.090,3.090,9.511) \quad \mathbf{w}_7 = \sqrt{2}/2$$
$$\mathbf{P}_8 = (0,3.090,9.511) \quad \mathbf{w}_8 = 1$$

Figure 23: The exact NURBS surface

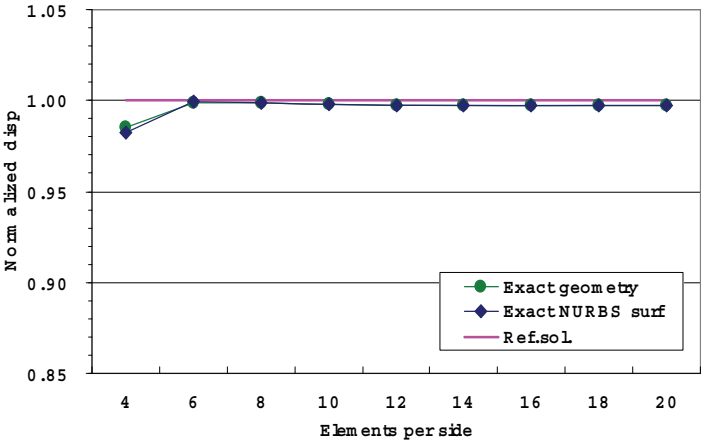

Figure 24: Convergence of normalized radial displacement

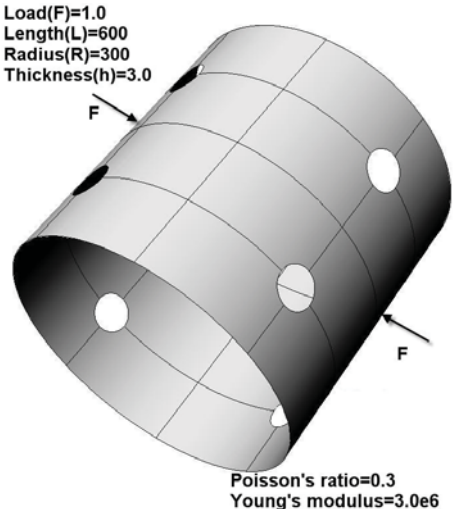

Figure 25: Trimmed cylindrical NURBS surface

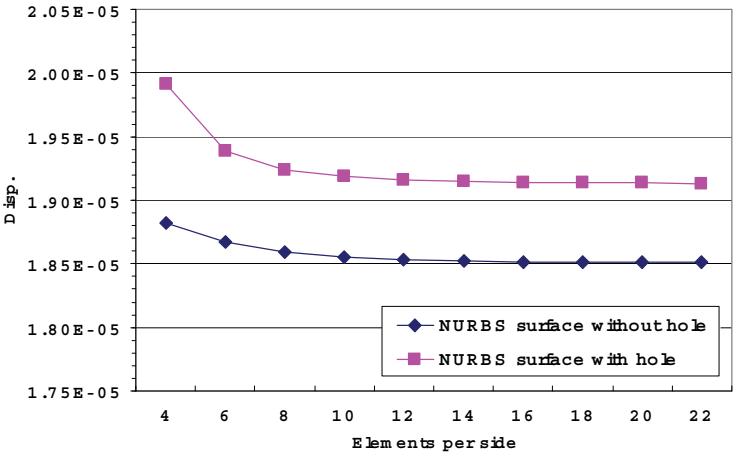

Figure 26: Convergence of radial displacement of cylinder surface

$$y(\theta^1,\theta^2) = r\sin(\theta^1)\cos(\theta^2)$$

$$z(\theta^1,\theta^2) = r\cos(\theta^1)$$

The analysis results of the exact NURBS surface and the analytically exact geometry are almost the same as those shown in Fig. 24. This means that the NURBS equation can guarantee about the same results as the analytically exact geometry can for quadratic surfaces.

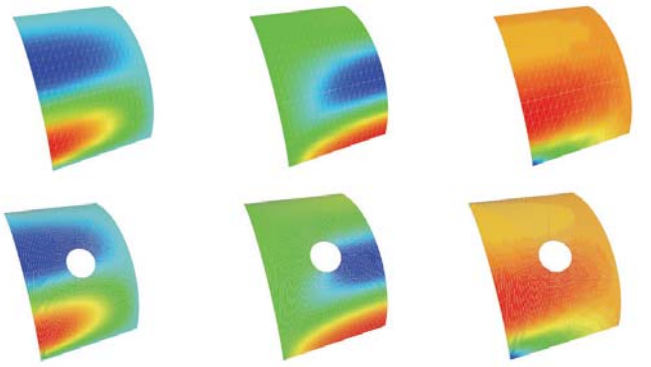

(a) u -direction (b) v -direction (c) w -direction

Figure 27: Displacement distribution

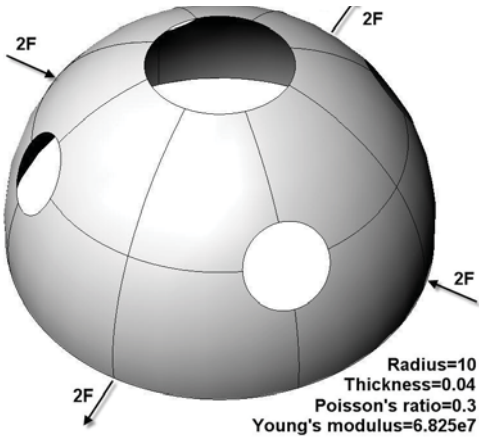

Figure 28: Trimmed hemi-spherical NURBS surface

4.3 Case 3: Trimmed Surfaces

A trimmed NURBS surface is defined by a set of trimming loops together with the NURBS surface itself. Each trimming loop consists of a set of NURBS curves, which are defined over the parametric space of the NURBS surface. The trimmed surface is often encountered during the modeling in the CAD systems and the most common one results from the intersection between two surfaces. The resulting intersection curve is a curve on the surface of either of the two surfaces. To verify the developed geometrically exact shell element and linkage framework with a CAD

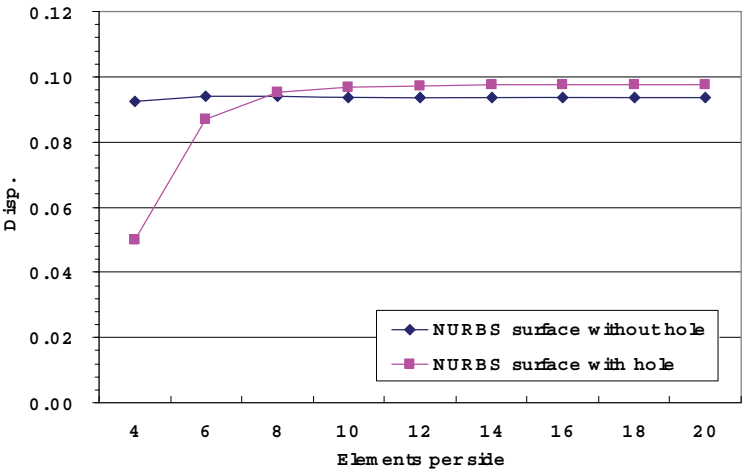

Figure 29: Convergence of radial displacement of cylinder surface

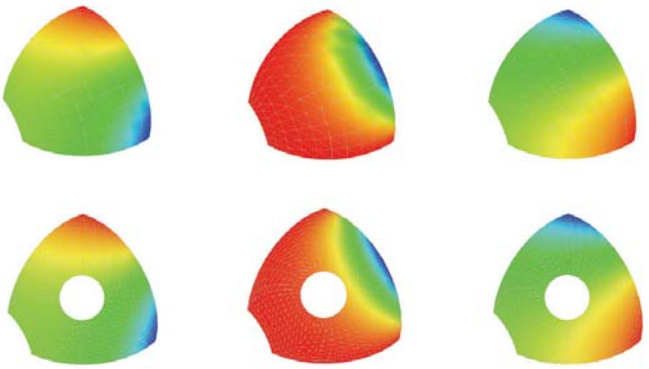

(a) u -direction (b) v -direction (c) w -direction

Figure 30: Displacement distribution

system, two examples will be introduced here. One is a cylindrical surface with a hole on its surface (Fig.25) and the other is a hemispherical surface having a hole (Fig.28). All geometry and material properties are the same as those of the previous examples, except that these surfaces have cutouts. These surfaces are modeled in the CAD system and our developed program imports the surfaces in IGES format file. The analysis result shows very good convergence even for a relatively coarse

mesh is used. (Fig.26, 29)

5 Conclusions

In this study, we set up a framework that directly links a general tensor-based geometrically exact shell finite element to the NURBS surface geometric modeling. By using the NURBS representation, we can use the present general tensor-based shell element to describe an arbitrary geometry of free-form surfaces, including the trimmed surfaces as well as quadratic cylindrical, conical and spherical surfaces, which can be exactly represented by the NURBS equation. Some numerical examples verified this property. The geometrically exact shell element formulated in the parametric domain with the NURBS equation provides an efficient linkage framework between the surface modeling of CAGD (Computer Aided Geometric Design) and finite element analysis.

Several numerical examples demonstrated the validity and efficiency of the developed geometrically exact shell element and the successful integration of the proposed shell element with the geometric modeling based on the NURBS equation. The performance of developed shell element was improved by employing the bubble shape functions as well as the membrane and shear lockings were considerably alleviated by the assumed strain methodology. The developed linkage framework employing the NURBS equation has various applications and functionality for the analysis of general shell surfaces. Trimmed surfaces with some cutouts on the surface were also considered to enlarge the scope of applications.

Acknowledgement: This work was supported by the Korea Science and Engineering Foundation(KOSEF)grant funded by the Korea government(MOST) (No. ROA-2007-000-20109-0).

Reference

Ahmad S.; Irons B.M.; Zienkiewicz O.C. (1970): Analysis of thick and shell structures by curved finite element. *International Journal for Numerical Methods in Engineering*, Vol.2, pp.419-459.

Basar Y.; Kintzel O. (2003): Finite Rotations and large Strains in Finite Element Shell Analysis, *CMES: Computer Modeling in Engineering & Science*, Vol.4, No.2, pp.217-230.

Bathe K.Y.; Dvorkin E.M. (1986): A formulation of general shell elements, the use of mixed interpolation of tensorial components, **Int.J.Numer. Methods Engrg.**, Vol.22, pp.697-722.

Budiansky B.; Sanders J.L. Jr. (1963): On the "best" First-Order Linear Shell Theory. *Prog. Appl. Mech.*, Vol.20, pp.129-140.

Cho M.; Roh H.Y. (2003): Development of Geometrically Exact New Shell Elements Based on General Curvilinear Coordinates, *International Journal for Numerical Methods in Engineering*, Vol.56, No.1, pp.81-115.

Cho M.; Jun S. (2004): r-Adaptive mesh generation for shell finite element analysis, *Journal of Computational Physicsm*, Vol.199, No.1, pp.291-316.

De Boor C. (1972): On calculating with B-Splines, *J. Approx. Theory*, Vol.6, pp.50-62.

De Boor C. (1978): *A Practical Guide to Splines*, New York: Springer-Verlag.

Farin G. (1993): *Curves and Surfaces for Computer Aided Geometric Design: a Practical Guide*, Academic Press, New York.

Green A.E.; Zerna W. (1968): Theoretical Elasticity. Oxford University Press.

Jarak T.; Soric J.; Hoster J. (2007): Analysis of Shell Deformation Responses by the Meshless Local Petrov-Galerkin(MLPG)Approch, *CMES: Computer Modeling in Engineering &Science*, Vol.18, No.3, pp.235-246.

Lee E.T.Y. (1989): Choosing nodes in parametric curve interpolation, *CAD*, Vol.21, pp.363-370.

Lee K.; Cho C.; Lee S.W. (2002): A geometrically Nonlinear Nine-Node Solid Shell Element Formulation with Reduced Sensitivity to Mesh Distortion, *CMES: Computer Modeling in Engineering&Science*, Vol.3, No.3, pp.339-349.

Lee S.W.; Wong S.C.; Rhiu J.J. (1985): Study of a nine node mixed formulation finite element for thin plates and shell, *Comput.Struct*, Vol.21, pp.1325-1334.

Naghdi P.M. (1963): Foundations of Elastic Shell Theory. *Progress in Solid Mechanics 4*, Edited by Sneddon, I.N. North-Holland.

Piegl L.; Tiller W. (1997): *The NURBS Book*, Springer-Verlag, New York, NY Second Edition.

Rhiu J.J.; Lee S.W. (1987): A new efficient mixed formulation for thin shell finite element models, *Int. J. Methods Engrg.*, Vol.24, pp.581-604.

Roh H.Y.; Cho M. (2004): The application of geometrically exact shell elements to B-spline surfaces, *Computer Meth. Appled Mech and Engrg*, Vol.193, pp.2261-2299.

Roh H.Y.; Cho M. (2005): Integration of geometric design and mechanical analysis using B-spline functions on surface, *International Journal for numerical methods in engineering*, Vol.62, No.14, pp.1927-1949.

Shaw A.; Banerjee B.; Roy D. (2008): A NURBS-based Parametric Method

Bridging Mesh-free and Finite Element Formulation, *CMES: Computer Modeling in Engineering & Science*, Vol.26, No.1, pp.31-57.

Simo J.C.; Fox D.D. (1989): On a stress resultant geometrically exact shell model. Part I: Formulation and Optimal Parameterization, *Comput. Methods Appl. Mech. Engrg.*, Vol.73, pp.267-304.

Simo J.C.; Fox D.D.; Rafai S. (1989): On a stress resultant geometrically exact shell model. Part II: The linear theory; computational aspects, *Comput. Methods Appl. Mech. Engrg.*, Vol.73, pp.53-92.

Sladek J.; Slade V.; Wen P.H.; Aliabadi M.H. (2006): Meshless Local Petrov-Galerkin(MLPG) Method for Shear Deformable Shells Analysis, *CMES: Computer Modeling in Engineering & Sciences*, Vol.6, No.2, pp.103-117.

SMLib TM; NLib™, Solid Modeling Solutions, Inc. `http://www.smlib.com/`.

Stander N.; Matzenmiller A.; Ramm E. (1989): An Assessment on assumed strain methods in finite rotation shell analysis, *Engrg. Comput.*, Vol.3, pp.58-66.

Xiang J.; Chen X.; Yang L.; He Z. (2008): A Class of Wavelet-based Flat Shell Elements Using B-spline Wavelet on the Interval and Its application. *CMES: Computer Modeling in Engineering & Science*, Vol.23, No.1, pp.1-12.